FINAL REPORT

NASA CONTRACT NAG3 - 1343

Submitted to: Dr. Vernon Heinen
Electron Beam Technology Branch
Lewis Research Center
Cleveland, Ohio 44135

Submitted by: Dr. Jerry D. Cook
Department of Physics
Eastern Kentucky University
Richmond, Kentucky 40475

THE

RESONATOR

HANDBOOK

Prepared by: Shiliang Zhou
Department of Physics
Eastern Kentucky University
Richmond KY 40475

TABLE OF CONTENT

INTRODUCTION

The use of open resonators to measure electro-optical properties of dielectric samples and surface resistivities of metallic thin films has been recently extended into the submillimeter-wavelength region. A primary study was devised by Cook *et al.*[1] with a scanning hemispherical open resonator scaled to operate at these frequencies. In their work, a resonator cavity is fed by a far-infrared laser operating at 337 GHz. A second study[2] by that group has found that spurious modes were introduced into the cavity by samples with large radii. A simple method of using small samples with radii on the order of a beam waist was suggested to eliminate those spurious modes. This is important as these spurious modes can be confused with the Gaussian modes typically used in studies of an open resonator. Unfortunately, a resonator theory does not exist for cavities in which the dimension of a planar mirror is compatible with the beam waist. This creates problems when the only samples available are very small. Samples include dielectric substrates that would be small due to expense or availability (for example, type-IIa diamond). This means it is necessary to establish a sound theoretical basis for using the open resonator with a small planar mirror to make electrical and/or optical measurements.

Resonator methods make use of the change in cavity quality Q (discussed later) and change in resonant length to measure metallic surface resistivities and complex dielectric permittivities. Typically, at wavelengths larger than 10 mm (< 30 GHz), classical closed cavities have been used in these measurements. At some short-millimeter wavelengths, the small size required for these microwave resonant closed cavities has limited the ability to mechanically construct cavities. As we approach still shorter-millimeter wavelengths, it first becomes inconvenient and eventually impractical to prepare samples for closed cavities. An open hemispherical resonator has been proposed (see Ref. 1) as an alternative to the waveguide in the investigation of the characterization of material properties at higher frequencies, in particular, in the region between 337 GHz and 2.7 THz. Since these frequencies lie between the optical and microwave regions, the open resonator is an attempt to combine useful techniques from both regimes.

In the aforementioned studies, the measurements of the surface resistivity or dielectric constant were made by placing samples on the planar mirror in the hemispherical resonator. The energy dissipated or lost in the cavity is mainly in the conducting surfaces[3] while total stored energy depends on the geometrical dimension of the resonator. Jones[4]

adapted the Gaussian beam formula for use with a hemispherical resonator and described theoretical calculations of cavity Q, which can be obtained from the usual electromagnetic fields theory.

In order to theoretically predict accurate Q values, it is important to be able to calculate the exact total energy stored in an open resonator. In the hole-coupling approach in the experiments performed by Cook *et al.* (see Ref. 1) where a laser feeds the scanning resonant cavity through a small hole centered in the spherical mirror, the energy loss through a coupling hole should also be considered in measuring the Q factor of the cavity. They estimate a 2% error in calculating total energy in their work.

The purpose of this work is to extend resonator theory into the region in which the planar mirror is quite small. Results of the theoretical description are then extended to resonator design and experimental arrangements as discussed in further sections of this work. Finally, a discussion of dielectric measurements for small samples is included as a specific application of this work.

1. Review of open resonator theory

Before discussing specific applications, it is first necessary to review existing theories of open resonators. An open-resonator system uses two metal reflectors to form a resonant structure similar to that of a Fabry-Perot etalon. In making measurements such as surface resistivity or dielectric constant, the open resonator is of the hemispherical type and consists of one spherical and one planar mirror separated by a distance slightly less than the radius of curvature of the curved mirror as shown in Figure 1. This figure shows a typical open resonator with dimensions scaled for the submillimeter-wavelength region. Figure 1 also shows a Gaussian field stored in the cavity. This field is characterized by a beam waist w_o.

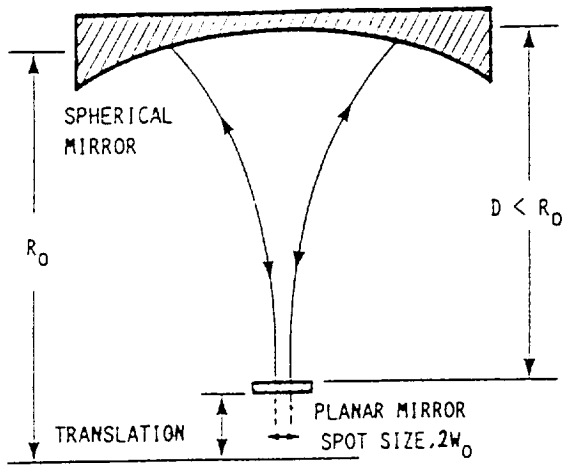

Fig.1. The hemispherical type of open resontor

This structure has several advantages. First, it is easily aligned. In fact, small misalignments can be ignored. Second, the experimental setup is easily arranged. Also, the beam waist is on the planar mirror, which serves as a sample. Furthermore, this system has a high cavity quality factor, or Q, defined as 2π times the ratio of the time-averaged energy stored in the cavity to the energy loss per cycle. The mode configurations of open resonators are characterized by the Kirchhoff-Fresnel diffraction theory[5] of electromagnetic radiation in which the electric field (or the magnetic field) is represented by a single scalar function E as described below. In view of the importance of this theory, and its relevance to this work, the derivation will be sketched here. The following derivation is based on the descriptions given by Kogelnik and Li[6] and Maitland and Dunn[5].

1.1 Spatial field distribution in open resonators

The scalar theory leads to the scalar wave equation (Helmholtz):

$$\nabla^2 E + k^2 E = 0 \qquad (1.1)$$

where $k=2\pi/\lambda$ is the propagation constant in free space and $E=E(x,y,z)$ is the scalar field, describing a wave travelling in the +z direction. (For convenience time variation has been

ignored.) A travelling wave solution to the electromagnetic wave equation should be of the form:

$$E(x,y,z)=\Psi(x,y,z)\exp(-jkz) \qquad (1.2)$$

where $\Psi(x,y,z)$ is an unknown amplitude function to be determined by substituting Eq. (1.2) into Eq. (1.1). The complete expression for travelling solutions are found (see Ref. 5) to take the form:

$$E(x,y,z)=E_0(w_0/w)\,[H_m(\sqrt{2}x/w)\,H_n(\sqrt{2}y/w)\exp(-r^2/w^2)\,]$$
$$\cdot\exp[-j(kz+\phi)-jkr^2/2R] \qquad (1.3)$$

The terms in the square brackets in Eq. (1.3) describe the transverse amplitude variation of the beam. H_m and H_n are Hermite polynomials which describe variations of the E_{mn} mode in the x and y directions, respectively. r is the transverse distance from the z axis.

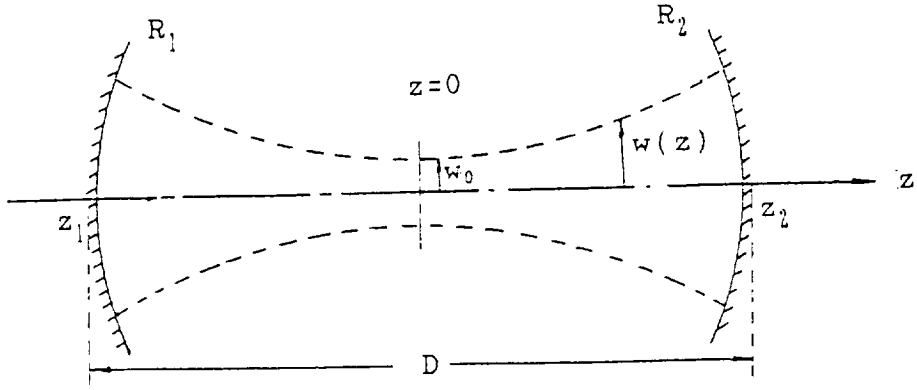

Fig.2. An open resonator showing the beam geometry

Figure 2 geometrically shows the relationship between w and w_o in Eq. (1.3). $w=w(z)$ is the radius parameter of the beam given by

$$w^2=w_o^2[1+(2z/kw_o^2)^2] \qquad (1.4)$$

where w_o is the minimum radius at the waist of the beam and is determined by boundary conditions. The distance of the beam from the origin ($z=0$) is z which can be expressed in terms of the parameters of the cavity[5]. For z_1 and z_2 in Figure 2, we consider the Gaussian beam as the primary mode of a resonant cavity formed from two spherical mirrors (radii of curvature R_1 and R_2) with a distance D apart. They are given by

$$z_1=-(R_2-D)D/(R_1+R_2-2D) \qquad (1.5)$$

$$z_2=(R_1-D)D/(R_1+R_2-2D) \qquad (1.6)$$

The term $\phi=\phi(z)$ describes a phase change on the axis of the beam given by

$$\phi=(1+m+n)\tan^{-1}(kw_o^2/2z) \qquad (1.7)$$

In the argument of the final exponential of Eq. (1.3), $R=R(z)$ is the radius of curvature of the wavefront. It is given by

$$R=z[1+(kw_o^2/2z)^2] \qquad (1.8)$$

R becomes infinite (i.e. describes a plane wavefront) at the waist. At the reflectors, R is equal to the radius of curvature of the reflectors R_1 and R_2. This condition determines w_o,

$$(kw_o^2)^2=4(R_1-D)(R_2-D)(R_1+R_2-D)D/(R_1+R_2-2D)^2 \qquad (1.9)$$

In the hemispherical cavity, R_2 is slightly larger than D and R_1 goes infinite. Eq. (1:9) reduces to

$$(kw_o^2)^2=4(R_2-D)D \qquad (1.10)$$

Mathematical superposition of forward and reverse traveling beams of similar mode and the fitting of the resulting standing wave to the boundary conditions at the reflectors gives the field description of the TEM_{mnq} mode resonances, where m,n=0,1,2... refer to variation in the x,y-directions and specific transverse modes. q is an integer typically much greater than 1 and describes longitudinal modes.

For the cavity to resonate, the phase shift when the beam travels from one mirror to the other must be an integral multiple of π because only in this case will a field be established inside the cavity with a well defined phase structure. Using the phase term of Eq. (1.3) for the phase shift per transit, along the z-axis (r=0), we have the

following condition for resonance:

$$kz_2+\phi(z_2)-[kz_1+\phi(z_1)]=q\pi \qquad (1.11)$$

where q is an integer which equal to the number of the standing waves in the cavity. Inserting Eq. (1.5), (1.6), and (1.7) into Eq. (1.11), one obtains

$$kD=q\pi+(1+m+n)\tan^{-1}\sqrt{D(R_1+R_2-D)/(R_1-D)(R_2-D)} \qquad (1.12)$$

The resonant frequency of the resonator for the TEM_{mnq} mode is given by

$$f_{mnq}=c[q\pi+(1+m+n)\tan^{-1}\sqrt{D(R_1+R_2-D)/(R_1-D)(R_2-D)}]/2\pi D \qquad (1.13)$$

and the resonant length D is

$$D=c[q\pi+(1+m+n)\tan^{-1}\sqrt{D(R_1+R_2-D)/(R_1-D)(R_2-D)}]/2\pi f_{mnq} \qquad (1.14)$$

Since the radius R_1 goes infinite in the hemispherical resonator, from Eq. (1.13) one therefore obtains the resonant frequency:

$$f_{mnq}=c[q\pi+(1+m+n)\tan^{-1}\sqrt{D/(R_2-D)}]/2\pi D \qquad (1.15)$$

1.2 Resonator without sample

By definition the cavity quality Q can also be written as

$$Q=f(\text{energy stored})/(\text{power dissipated per radian}) \quad (1.16)$$

where f is the radiation frequency. The total electromagnetic energy density is denoted by

$$u=(\varepsilon_o E^2+\mu_o H^2)/2 \quad (1.17)$$

where ε_o and μ_o are electric permittivity and magnetic permeability in the vacuum, E is the electric field intensity, and H is the magnetic field intensity. For any transverse electromagnetic or TEM wave, the electric and magnetic energy densities are equal,

$$\varepsilon_o E^2/2=\mu_o H^2/2 \quad (1.18)$$

and the total energy density is therefore $\varepsilon_o E^2$. If losses due to diffraction or coupling hole are neglected, then the energy stored in an empty resonator is expressed as

$$W_o=\varepsilon_o \int_v <E^2> dv \quad (1.19)$$

where dv in cylindrical coordinates is expressed as $2\pi r dr dz$,

V is the total volume of the cavity, and the time average term $\langle E^2 \rangle$ is $E \cdot E^*/2$. Since only the fundamental mode is considered, m=n=0 and both Hermite polynomials reduce to unity. The term $\exp(-r^2/w^2)$ in Eq. (1.3) describes the dominant Gaussian profile of the beam. Thus

$$\langle E^2 \rangle = [E_o^2 w_o^2 (\exp(-2r^2/w^2)/w^2(z))]/2 \qquad (1.20)$$

Substituting Eq. (1.20) into Eq. (1.19) gives

$$W_o = [\varepsilon_o E_o^2 w_o^2 \int_V (\exp(-2r^2/w^2)/w^2(z)) dv]/2 \qquad (1.21)$$

$$= \pi \varepsilon_o E_o^2 w_o^2 \int_o^D [\int_o^\infty (\exp(-2r^2/w^2)/w^2(z)) r dr] dz \qquad (1.22)$$

In Eq. (1.22), the limits of integral of r go from zero to infinity, i.e. the cavity is considered to have infinite dimensions. Setting $x = r^2/w(z)^2$, we have

$$dx = 2rdr/w(z)^2 \qquad (1.23)$$

and

$$W_o = \pi \varepsilon_o E_o^2 w_o^2 \int_o^D [\int_o^\infty \exp(-2x) dx/2] dz \qquad (1.24)$$

$$= [\pi \varepsilon_o E_o^2 w_o^2 \int_o^D dz]/4 \qquad (1.25)$$

If the separation of the mirrors in the resonator is denoted by D, then

$$W_o = \pi w_o^2 \varepsilon_o E_o^2 D/4 \qquad (1.26)$$

Eq. (1.26) agrees with the expression given by Siegman[7] and differs from Jones (see Ref.4) by a factor of 2.

Now let us consider the energy losses in the metallic mirrors. The ratio of displacement current density $\partial D/\partial t$ to conduction current density J_f in a conductor can be estimated as[8]

$$|(\partial D/\partial t)/J_f| = 2\pi\varepsilon_o f/\sigma \tag{1.27}$$

We may set $\sigma=10^7$ ohms/meter for a good conductor, then

$$|(\partial D/\partial t)/J_f| \approx 10^{-17} f \tag{1.28}$$

where f is the radiation frequency. The displacement current in a good conductor is therefore negligible at any frequency lower than 10^{15} hertz. With this approximation, the Maxwell curl equation becomes

$$\vec{E}_c = \nabla \times \vec{H}_c/\sigma \tag{1.29}$$

where vectors $\vec{E}_c$ and $\vec{H}_c$ represent electromagnetic waves in the conductor. If $\vec{n}$ is the unit normal outward from the conductor and ξ is the normal coordinate inward into the conductor, then the gradient operator in Eq. (1.29) can be written as

$$\nabla = -\vec{n}\partial/\partial\xi \tag{1.30}$$

Since inside the conductor $\vec{H}$ is parallel to the surface, the solution for $\vec{H}_c$ is[9]

$$\vec{H}_c=\vec{H}_o\exp(-\xi/\delta)\exp(i\xi/\delta) \tag{1.31}$$

where H_o is the tangential magnetic field outside the surface and δ is the skin depth defined by

$$\delta=(1/\pi f\sigma\mu_o)^{1/2} \tag{1.32}$$

Inserting Eq. (1.30) and Eq. (1.31) into Eq. (1.29), we obtain

$$\vec{E}_c=(-\vec{n}x\partial\vec{H}_c/\partial\xi)/\sigma \tag{1.33}$$

$$=\{(1-i)\exp[(i-1)\xi/\delta]\vec{n}x\vec{H}_o\}/\sigma\delta \tag{1.34}$$

$$=R(1-i)\exp[(i-1)\xi/\delta]\vec{n}x\vec{H}_o \tag{1.35}$$

where $R=1/\sigma\delta$ is defined as the surface resistivity of the conductor. The time average power absorbed per unit volume is

$$p=(\vec{j}_f\cdot\vec{E}_c^{\,*})/2 \tag{1.36}$$

$$=\sigma\vec{E}_c\cdot\vec{E}_c^{\,*}/2 \tag{1.37}$$

$$=\sigma R^2\exp(-2\xi/\delta)H^2 \tag{1.38}$$

where "*" indicates the complex conjugate. The total power loss is

$$P=\int_L pA\,d\xi \tag{1.39}$$

where A is the area of the beam cross section πw^2 and L is the thickness of the conductor. Because L is much larger than δ, then Eq. (1.39) becomes

$$P=\int_o^{\infty} p\pi w^2 d\xi \tag{1.40}$$

$$=RH_o^2\pi w_o^2/2 \tag{1.41}$$

$$=R\pi w_o^2 E_o^2/2Z_o^2 \tag{1.42}$$

where $Z_o=(\mu_o/\varepsilon_o)^{1/2}$ is the impedance of free space. The net power P_t loss in the resonator is given by

$$P_t=P_c+P_p=\pi w^2 E^2 (R_c+R_p)/2Z_o^2 \tag{1.43}$$

$$=\pi w_o^2 E_o^2 R_c (M+1)/2Z_o^2 \tag{1.44}$$

where M is R_p/R_c and subscripts p and c indicate the planar mirror and concave mirror, respectively. From Eq. (1.16), the Q factor of the empty resonator is finally given by

$$Q_o=fW_o/P_t \tag{1.45}$$

$$=fD\varepsilon_o Z_o^2/2R_c(M+1) \tag{1.46}$$

2. Small samples consideration

We now extend the theory to cover situations where the planar mirror is quite small. When making measurements of surface resistivities of metallic materials, samples are used as planar reflectors to form one mirror of the empty resonator. Some samples are small due to expense and availability so that modifications of resonator theory are required. The results can then be applied to a resonator loaded with small dielectric samples. The complex dielectric constants of these samples can be extracted from such measurements.

2.1 Spurious modes in the hemispherical cavity

The theory used by Jones[10] applies only to the Gaussian TEM_{ooq} modes supported in the cavity. Resonant frequencies other than the TEM_{ooq} modes were given by Eq. (1.15). Those resonances were attributed to spurious (higher-order) modes and had been ignored since they were sufficiently separated from the Gaussian mode. However, the experiment performed by Cook *et al.* (see Ref. 2) has shown that the spurious modes are not negligible as the sample radius is enlarged. These spurious modes may lead to confusion in the resonator cavity, where higher-order modes from frequencies other than the Gaussian resonant frequency could be supported. To prevent the introduction of spurious modes within the resonant cavity,

it was suggested (see Ref. 2) that the radius or effective sample size of the planar mirror could be reduced into a working radius slightly larger than the Gaussian beam spot w_o. This size, while large enough to support the desired Gaussian TEM_{ooq} mode, is small enough to prevent the occurrence of higher-order modes. However, it is not clear that existing resonator theory is adequate for this application. We next address this question.

2.2 Modification of the theory

To proceed further we must investigate two situations: (1) The small sample does not affect the electric field distribution in the cavity so that the field of the fundamental modes is an exact Gaussian beam, and (2) the consequent possibility of diffraction losses can still be neglected.

In an open resonator formed by a hemispherical cavity, fundamental TEM_{ooq} modes have Gaussian profiles and the electric field varies in the radial direction as

$$E(x,y,z)=E_o(w_o/w)\exp(-r^2/w^2)\exp[-j(kz+\phi)-jkr^2/2R) \qquad (2.1)$$

Since the small sample serves as a planar mirror, assumption (1) is valid as long as the sample is mounted without misalignments in the cavity and large enough to support the Gaussian Mode. The beam radius w given by Eq. (1.4) varies

parabolically along the axis having a minimum value, w_o, at the waist (z=0) of the resonance. In experimental arrangements, the sample is placed in the position of the beam waist in the hemispherical cavity and its size is sufficiently larger than the beam waist w_o so as to prevent "leakage". Assumption (2) is also true since the Q factor of the resonator due to the diffraction loss was estimated to be over 10^7 in these experiments[11] while the measured Q factors (given in Table 1 of section 3.5) have values on the order of 10^5. The diffraction loss in the cavity is therefore negligible compared to the conductor losses.

Reported measurements from Jones (see Ref. 10) are based on the hemispherical cavity in which the sample diameters were often in the range of 70-80 mm. These diameters are much larger than those of the Gaussian beam in the resonator. The Jones' theory assumes that the electric field is negligible for transverse distances much larger than the beam waist w_o. When the sample is of a small radius compatible with the beam waist w_o, this assumption no longer holds.

To accurately calculate the Q factor of the cavity, we first modify the stored energy expression (1.22). Consider the hemispherical cavity shown in Figure 1. The total energy stored in an open infinite cavity is given by Eq. (1.19). For the empty resonator with a small planar mirror, the integral of r does not go to infinity in Eq. (1.22). Thus

$$W_o=\varepsilon_o E_c^2 w_c^2 \int_c^D [\int_c^r (\exp(-2r^2/w^2)/w^2(z))\, r dr]\, dz \qquad (2.2)$$

$$=[\pi\varepsilon_o E_c^2 w_c^2 \int_c^D (1-\exp(-2r^2/w^2))\, dz]/4 \qquad (2.3)$$

When r is much larger than w, we find W_o equals $\pi\varepsilon_o E^2 w^2 D/4$ as shown in Eq. (1.26). In the case of small samples, the transverse distance r in the resonator is just a little larger than the beam radius w. By setting r=bw (b>0), where b is a scaling constant, from Eq. (2.3) we can see that

$$W_o'=\pi\varepsilon_o E_c^2 w_c^2 D[1-\exp(-2b^2)]/4 \qquad (2.4)$$

or

$$W_o'=W_o[1-\exp(-2b^2)] \qquad (2.5)$$

Eq. (1.46) is then changed into

$$Q_o'=Q_o[1-\exp(-2b^2)] \qquad (2.6)$$

The theoretical curve from Eq. (2.5) is shown in Figure 3. In this figure, we see that the ratio of the corrected energy W_o to the uncorrected energy W_o is very close to 1 as long as r is not smaller than 1.5w.

The importance of this result can be summarized as follows;

(1) At the point of r/w=1.5 in Figure 3, the corrected energy W_o is $0.9889W_o$. Thus, for the sample size slightly larger than $1.5w_o$, the energy leakage can be ignored while the spurious modes have been effectively repressed.

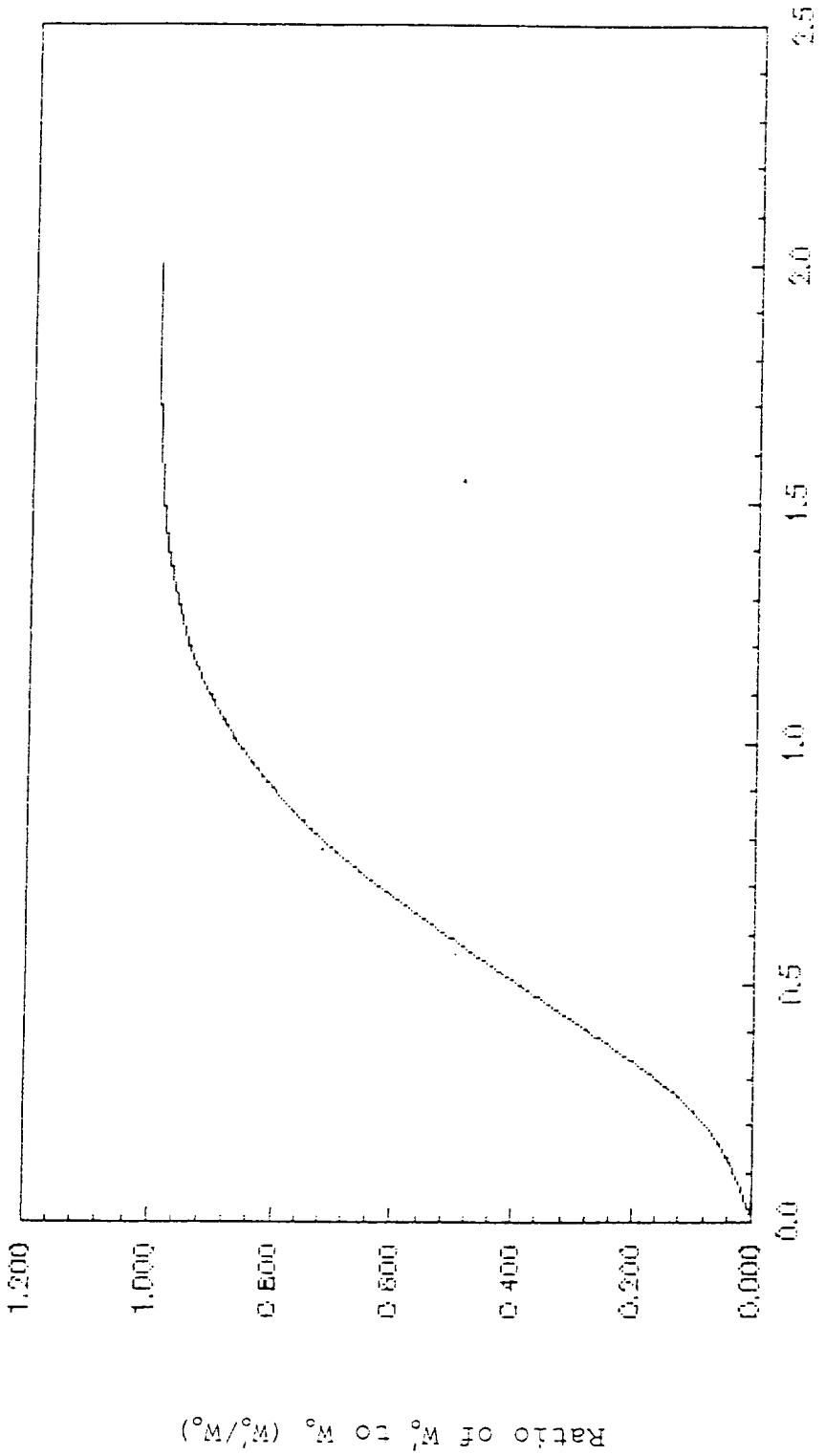

Fig.3. The corrected energy stored in the cavity as a function of planar mirror sizes

(2) This has the practical advantage of permitting samples of smaller radius to be used in measurements since the beam radius w has its minimum value w_o at the planar mirror in the hemispherical resonator.

(3) The Q-factor of cavities containing small samples can be more precisely predicted since we know the exact energy stored in the cavity.

Before one can optimize the design of an open resonator to suit it to a particular application, it is important to note the experiment result given by Cook *et al.* (see Ref. 2). The experiment is performed at 337 GHz with R_2=135.9 mm and D=135.5 mm. Their work shows that spurious modes are prevented when the radius of the sample is smaller than 5 mm. The beam waist can be obtained by Eq. (1.10). It gives $w_o \approx 1.5$ mm. Using the theoretical results for the consideration of no energy leakage in the cavity, we can select the sample radius in the range of $1.5w_o$ ($\approx$2.3 mm) to 5 mm.

It should be pointed out that Eq. (2.6) must be used to give precise measurements when the sample radius is smaller than $1.5w_o$. However, the diffraction loss in such small samples may not be neglected. The magnitude of the diffraction loss can be estimated (see Ref. 11) in determining the Q factor of the resonator. This diffraction limits the effective size of planar samples to about $1.5w_o$.

2.3 Resonator containing dielectric sample

The open resonator used in making precise measurements of permittivity and loss angle (discussed later) for a range of dielectric materials is mainly the hemispherical type developed by Jones (see Ref. 10). A "loaded" hemispherical resonator consisted of a planar mirror and a concave mirror is shown in Figure 4.

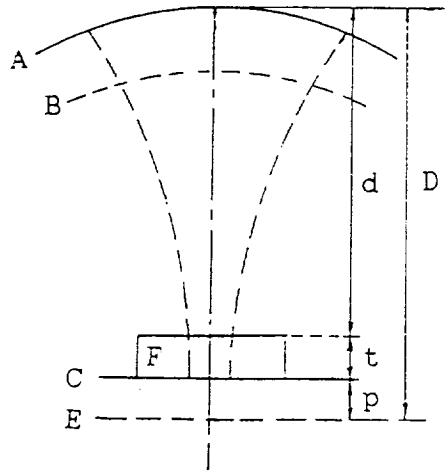

Fig.4. Hemispherical resonator

A=concave mirror

B=phase front

C=plane mirror at resonant position with sample

E=plane mirror at resonant position without sample

F=sample

After making the empty cavity into resonance, a dielectric sample of thickness t, with refractive index n, is loaded onto the planar mirror as indicated in Figure 4, a change p in length of the resonator is required to bring the system back into resonance. Following the theory describe by Jones (see Ref. 4), the stored energy expression (1.26) is

$$W_L=\pi w_o^2\varepsilon_o E_o^2(t\Delta+d)/4 \tag{2.7}$$

where $$\Delta=n^2/[n^2\cos^2(nkt-\phi_t)+\sin^2(nkt-\phi_t)] \tag{2.8}$$

and $$\phi_t=\tan^{-1}(2t/nkw_o^2) \tag{2.9}$$

Similarly, the Q-factor from Eq. (1.46) becomes

$$Q_L=f\varepsilon_o Z_c^2(t\Delta+d)/2R_c(M\Delta+1) \tag{2.10}$$

Considering the resonator with the small sample and following the calculations used for an empty resonator, Eq. (2.5) can be written as

$$W_L'=W_L[1-\exp(-2b^2)] \tag{2.11}$$

Correspondingly, Eq. (2.6) becomes

$$Q_L'=Q_L[1-\exp(-2b^2)] \tag{2.12}$$

The ratio of Q_L' to Q_o' is given by

$$Q_L'/Q_0' = Q_L/Q_0 = (M+1)(t\Delta+d)/(M\Delta+1)D \qquad (2.13)$$

or

$$Q_L' = Q_L'(M+1)(t\Delta+d)/(M\Delta+1)D \qquad (2.14)$$

This last equation will be used for calculating the loss angle later.

3. Using an open resonator for empirical dielectric measurements

Determination of dielectric properties of materials is a natural application for open resonators since easily measured parameters of the resonator, the resonant frequency f, resonant length D, and the Q factor, are simply related to the permittivity and loss of the included media. This chapter will cover two applications of the open hemispherical resonator.

3.1 Electromagnetic quantities

The complex refractive index $\tilde{n}$ is derived from complex dielectric permittivity $\tilde{\varepsilon}$ of Maxwell's equations so that

$$\tilde{\varepsilon}=\tilde{n}^2 \qquad (3.1)$$

The real and imaginary parts of $\tilde{n}$ are, by definition

$$\tilde{n}=n-i\kappa=n-i(\alpha c/4\pi f) \qquad (3.2)$$

where κ is the absorption index $\alpha c/4\pi f$, α the absorption coefficient in cm^{-1}, f the frequency in hertz, c the velocity of light in vacuum, and n the real refractive index. The complex dielectric permittivity ε has real and imaginary parts

expressed as

$$\tilde{\varepsilon}=\varepsilon'-i\varepsilon'' \qquad (3.3)$$

Then, our definitions provide us with the simple relationships between the fundamental optical quantities, α and n, and the dielectric quantities ε' and ε'', as follows

$$\varepsilon'=n^2-\kappa^2=n^2-(\alpha c/4\pi f)^2 \qquad (3.4)$$

$$\varepsilon''=2n\kappa=n\alpha c/2\pi f \qquad (3.5)$$

The term loss tangent, or as is commonly expressed, $\tan\delta$, is the ratio of the imaginary part ε'' to the real part ε' of the dielectric permittivity

$$\tan\delta=\varepsilon''/\varepsilon' \qquad (3.6)$$

Note that the expression for the dielectric constant ε' is not a constant. It contains a term inversely dependent on frequency. It is not a constant, that is, unless the second term that contains the frequency can be neglected. This is usually the case at optical frequencies where the denominator of the second term is very large. At millimeter wave frequencies, however, we cannot drop the second term unless the absorption coefficient α is sufficiently small compared with the refraction index n so that the real part of the dielectric permittivity ε' is effectively independent of frequency.

Specially, if the absorption coefficient is less than unity at 300 GHz, then ε' is truly a dielectric constant and the material is "low loss" in this case.

3.2 Open resonator method

Resonator methods make use of the change in Q and in resonant length to provide ε' and ε''. A convenient form of resonant structure is the hemispherical type that employs one concave and one planar mirror as shown in Figure 4. This geometrical consideration may allow measurements to be made on small diameter samples because the beam waist spot is on the planar mirror in the cavity. The sample placed on the planar mirror can be a liquid or a flat solid. Cullen and Yu[12], considering a sample of thickness t, have applied the beam wave theory to the open resonator containing a dielectric sample and have derived equations from which the refractive index n and tangent of loss angle δ can be obtained. These equations are

$$\tan(nkt-\phi_t)/n=-\tan(kd-\phi_d) \tag{3.7}$$

$$d=D-t-p \tag{3.8}$$

$$\phi_t=\tan^{-1}(2t/nkw_c^2) \tag{3.9}$$

$$\phi_d=\tan^{-1}[2(d+t/n^2)/kw_c^2]-\tan^{-1}(2t/n^2kw_c^2) \tag{3.10}$$

$$kw_c^2=2[(d+t/n^2)(R_o-d-t/n^2)]^{1/2} \tag{3.11}$$

where p is the change in length of the resonator required to bring the system back into resonance after the sample has been inserted. ϕ_t and ϕ_d arise from the extra phase shift due to the fact that we have a Gaussian beam in the resonator and not a plane wave. The permittivity $\varepsilon'=n^2$ is then obtained by solving Eq. (3.7) for n.

The tangent of the loss angle δ is given by

$$\tan\delta=Q^{-1}[(t\Delta+D)/(t\Delta+2k^{-1}\sin 2(kd-\phi_d)] \qquad (3.12)$$

where $$\Delta=n^2/[n^2\cos^2 nkt-\phi_t)+\sin^2(nkt-\phi_t)] \qquad (3.13)$$

Q_e is the Q factor of the resonator considering only energy loss in sample. In open resonators each contribution to the resonant mode losses can be described in terms of individual Q-factors, Q_i, which combine in parallel to give the overall resonator Q-factor, $Q=1/(\Sigma Q_i)$. Let Q_d be the measured Q-factor for the resonator containing the sample and Q_L the calculated Q factor for the resonator containing an ideal loss free sample of the same dimension and permittivity as the real sample. Q_L is given by

$$Q_L=Q_o(M+1)(t\Delta+d)/(M\Delta+1)D \qquad (3.14)$$

where Q_o is the measured Q factor of the empty resonator. Thus Q_e can be calculated by

$$1/Q_e=1/Q_d-1/Q_L \qquad (3.15)$$

The above theory assume that the upper surface of the sample is slightly convex as shown in Figure 5 (a) to match the phase front of the beam in the resonator. This means that for the plane parallel sample used in practice the small volume shown shaded in Figure 5 (b) is unaccounted for the theory.

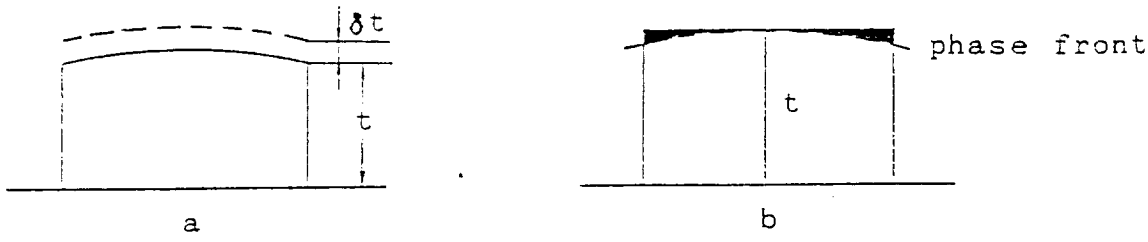

Fig.5. Mismatch at sample surface

Jones[13] has shown that a satisfactory method of correcting for the extra volume is to calculate the amount of stored energy in this volume and to estimate by how much the sample thickness must be increased from t to t+δt so that the stored energy in the thickness δt is the same as that in the shaded volume. This procedure conserves the total energy in the resonator. The term δt is given by

$$\delta t = w(t)^2/4R(t) \qquad (3.16)$$

where w(t) and R(t) are, respectively, the beam radius and the radius of curvature of the phase front at z=t. If a new value of t′=t+δt is used instead of t in Eqs. (3.7) to (3.11), then accurate values for ε′ and tanδ are obtained.

3.3 Experimental arrangement

Developing a mechanism to effectively feed and monitor the energy stored in an open resonator is critical in making measurements of metallic surface resistivities and dielectric constants. The experimental hole-coupling geometry fed by an optically pumped far infrared laser is used as shown in Figure 6. This experiment was performed by Cook *et al.*. The theoretical analysis of the data is dependent on the fundamental mode; higher mode degeneracies must be avoided as we mentioned before.

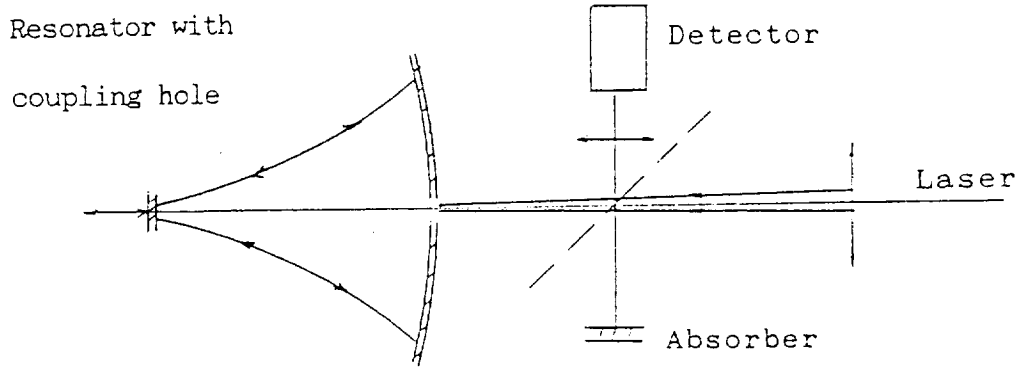

Fig.6. The experimental apparatus

The resonator cavity was excited by the output from an Apollo Model 122 FIR laser at NASA Lewis Research Center, operating with a Gaussian TEM_{00} mode at 337 GHz. In this arrangement the incident beam and exit beam are separated so

that only energy that leaked out from the cavity through the coupling hole was monitored. The 2-mm-diameter coupling hole should contribute losses of about 2% to the energy stored in the Gaussian field in the cavity[7]. Therefore, Eq. (1.46) should be multiplied by the factor 0.98 in the theoretical calculation due to this coupling hole loss. In our reference cavity both mirrors are aluminum. The radius of curvature of the spherical mirror used in measuring metallic surface resistivities is 135.9 mm. The resonator length at the first resonance is just smaller than 135.9 mm (See Table 1). These parameters were calculated by using Eq. (1.10) to limit the beam waist w_o on the planar mirror to approximately 1.5 mm. When measuring properties of dielectric materials, the radius of curvature of the spherical mirror was changed to 113.82 mm, which decrease the beam waist w_o to less than 1.5 mm. In both experimental arrangements, the dimension of the spherical mirror is a little larger than 100 mm, about 2 times the size of the Gaussian field on the mirror surface. This large curved mirror insures that leakage around the mirror edge can be neglected. The planar mirror is masked by a 1/4" (6.4 mm) diameter aperture to prevent spurious modes in the cavity. This size fits the optimal range given in section 2.2.

3.4 Empirical determination of the cavity Q factor

A measure of the sharpness of response of the cavity to external excitation is the Q-factor of the cavity, defined by Eq. (1.17). By conservation of energy the power dissipated in ohmic losses is the negative of the time rate of change of stored energy. An initial amount of energy decays away exponentially with a decay constant inversely proportional to Q and the frequency separation Δf between half-power points determines the Q of cavity is

$$Q=f/\Delta f \tag{3.17}$$

Empirically, the Q factor can be found[14] from $D/\Delta D$ where ΔD is the length separation of half-power width versus cavity resonant length D. To show this, we use the resonant condition given by Eq. (1.14). It can also be written as

$$f_{mnq}=c\left[q\pi+(1+m+n)\cos^{-1}\sqrt{(R_2-D)/R_2}\right]/2\pi D \tag{3.18}$$

In the hemispherical resonator, D is very close to R_2 so that $\sqrt{(R_2-D)}/R_2$ much less than 1. If let $g=[(R_2-D)/R_2]^{1/2}$, the expression of $\cos^{-1}g$ in series is

$$\cos^{-1}g=(\pi/2)-g-(g^3/6)-\ldots\ldots\approx(\pi/2)-g \tag{3.19}$$

Then, introducing the fundamental mode TEM_{ooq} into the resonant condition, we have

$$f=c[q+1/2-g/\pi]/2D \tag{3.20}$$

$$=c[q+1/2-\pi^{-1}\sqrt{(R_2-D)/R_2}]/2D \tag{3.21}$$

For $\sqrt{(R_2-D)}/R_2 << 1$ and $q >>1$, Eq. (3.21) becomes

$$f\approx c(q+1/2)/2D \tag{3.22}$$

and resonant frequencies of the two half power points are

$$f_{1,2}=f\pm\Delta f/2=0.5c[(q+1/2)/(D\mp\Delta D)] \tag{3.23}$$

where the frequency separation Δf is given by

$$\Delta f=f_2-f_1=0.5c(q+1/2)\Delta D/(D^2-\Delta D^2/4) \tag{3.24}$$

$$\approx 0.5c(q+1/2)\Delta D/D^2 \tag{3.25}$$

Here we drop the term $\Delta D^2/4$ since $D^2/\Delta D^2$ was on the order of 10^{10} in our experiments. According to Eq. (3.17), we have

$$Q=\Delta f/f\approx\Delta D/D \tag{3.26}$$

Although it is difficult to make accurate measurements of two half-power points D_1 and D_2, the half-power width $\Delta D=D_1-D_2$ can be measured accurately.

3.5 Measurement of surface resistivities of metallic samples

Let Q_{o1} be the first measured value with mirrors made from same metallic material. This serves as a reference to compare other sample losses. An attempt was made to give these two mirrors similar surface treatments so that the resistivities would be the same. Assuming that M=1 in this case, we can calculate R_{c1} from Eq. (1.46). Using another different metallic sample serving as a planar mirror, we then get Q_{o2}. From Eq. (1.46), it is seen that the ratio of Q_{o1} to Q_{o2} is

$$Q_{o1}/Q_{o2}=(M+1)/2 \qquad (3.27)$$

which gives us a value of M. Since Q_{o1} and Q_{o2} can be measured in both cases, we therefore use M to calculate the sample resistivity R_{c2}.

Table 1 shows some sample surface resistivities that were calculated from Q values measured at 337 GHz. Note that these relative values are based on the literature values from aluminum. The literature values are calculated from scaled dc values for resistivity $1/\delta\sigma$, where δ and σ are the classical ac skin depth and dc conductivity, respectively. Therefore, the literature values should be considered only as rough or approximate values. On the other hand, the experiment can be considerably improved to limit experimental error on the order of 5% or lower (see Ref. 1).

Table 1. Surface resistivity of selected metals

Material	Q[a] 10^3	D (mm)	R(measured) (10^{-3} Ω)	R(Ref.) (10^{-3} Ω)
Aluminum	110	135.5	---	188[b]
Copper	140	135.0	107	149[b]
Tantalum	85	135.5	299	454[c]
304 Stainless	30	133.7	1191	979[c]
.5um thick Au	96	135.5	243	187[c]

a. From J. D. Cook *et al.* Rev. Sci. instrum. **62**, 2480 (1991)

b. From K. J. Button, "Infrared and Millimeter Waves", Academic, 1979, Vol.1, p. 237

c. Calculated from dc conductivity values in R. C. Weast and M. J. Astle, "Handbook of Chemistry and Physics", CRC, Cleveland, OH, 1975-76, 56th Ed., p. D-171

3.6 Dielectric permittivity measurements

The details of the apparatus which operates at 337 GHz have been shown in Figure 4. The sample was placed on the planar mirror. The resonant length D for an empty resonator can be calculated from a knowledge of the frequency and the radius of curvature of the concave mirror. This measurement together with the sample thickness t gives us the data required for the solving of Eq. (3.7) for n and hence ε' as shown in previous section.

3.6.1 Computational procedure

Experimental data supplied by Cook *et al.* are shown in Table 2. We use data of crystal quartz, sapphire, and diamond to illustrate our technique.

Table 2. Sample thickness and reduction in resonant length

Sample	t (mm)	p (mm)
Sapphire	0.508	0.352
Quartz	0.659	0.338
Diamond	0.250	0.353

The sample index n of refraction can be calculated with the given data t and p. Note that the correction of the sample thickness should be made in calculations according to Eq. (3.16). To find the numerical solution of Eq. (3.7) we use Math CAD's "solve block" in our calculation. Math CAD uses an iterative method to solve equations and inequalities in a "solve block". This iterative method starts with guess values for the variables to be solved and the constraints and it ends with variable values that satisfy the constraints. Our "solve block" is listed in Appendix. Table 3 shows the results obtained for quartz, sapphire, and diamond.

3.6.2 Analysis of results

Equation (3.7) gives multiple solutions of the sample index. The "true index" is found among these values by comparing these values to those from classical dispersion theory. The theory[15] applied to a set of lattice oscillators relates the dielectric constant ε to the characteristic oscillator parameters. In a spectral region where $f \ll f_j$, for all j, the expression for the real part of the dielectric constant given by Eq. (3.4) and Eq. (3.5) can be expanded to give

Table 3. Calculated results for quartz, sapphire and diamond

Sample	t(mm)	p(mm)	n(guess)	n_{val}	t_{val}[a]
Quartz	0.659	0.338	1.5	1.546	0.665
			2.0	2.250	0.664
			2.5	2.940	0.664
			3.0	2.940	0.664
			3.5	3.628	0.663
Sapphire	0.508	0.352	2.0	1.635	0.513
			2.5	2.458	0.513
			3.0	2.458	0.513
			3.5	3.288	0.513
			4.0	4.125	0.513
Diamond	0.250	0.353	1.5	----	----
			2.0	2.53	0.253
			2.5	2.53	0.253
			3.0	----	----
			3.5	----	----

a. t_{val} is determined by $t+w(t)^2/4R(t)$

$$\varepsilon' = n^2 - \kappa^2 \approx S_0 + (S_0 - \varepsilon_\infty)\lambda_0^2 f^2 \qquad (3.28)$$

$$\varepsilon'' = 2n\kappa \approx (S_0 - \varepsilon_\infty)\gamma_0 \lambda_0 f \qquad (3.29)$$

here $$S_0 = \varepsilon_\infty + \sum_j S_j = n_0^2 \qquad (3.30)$$

$$\lambda_0^2 = (S_0 - \varepsilon_\infty)^{-1} \sum_j S_j (1 - \gamma_j) f_j^{-2} \qquad (3.31)$$

and $$\gamma_0 = f_0^{-1} (S_0 - \varepsilon_\infty)^{-1} \sum_j S_j \gamma_j f_j^{-1} \qquad (3.32)$$

where S_j is the jth oscillator, f_j is the characteristic frequency, γ_j is the dimensionless, frequency-independent damping constant, ε_∞ is the high-frequency dielectric constant, and the S_0 is the zero-frequency or static dielectric constant. For transparent substances, such that $n^2 >> \kappa^2$, the formula for index of refraction derived from Eq. (3.28) is

$$n \approx n_o + (n_o^2 - \varepsilon_\infty) n_o^{-1} \lambda_o f^2 / 2 \qquad (3.33)$$

By plotting experimental data for n vs. f^2 one should obtain a straight line according to Eq. (3.33). The values of n_o and λ_o may be determined from the intercept and slope of this line, provided that n_∞ is estimated from independent data in visible light. Roberts and Coon[16] gave a theoretical discussion and experiment results at a wavelength range from 40μ to 300μ using a grating monochromator for the determination of the indexes of quartz and sapphire. Their results, extrapolated to the low frequency of about 30 GHz, are: $n_\perp = 2.102$, $n_\parallel = 2.153$ in quartz and $n_\perp = 3.060$, $n_\parallel = 3.402$ in sapphire. Since quartz and sapphire are anisotropic materials, we use $n_\perp$ and

$n_{\parallel}$ to represent the crystal having its optical axis perpendicular or parallel to the surface. For low loss materials we do not expect any significant dispersion between the low-frequency values and the measurements carried out at 337 GHz. Hence, we compared our results and the values obtained from the literature. Taking these values as reference, we find 2.250 for quartz and 3.288 for sapphire from Table 3 are the correct values of these indexes. The index of diamond as found from Table 3 is unique. Van Camp *et al.*[17] provided the literature value n=2.36 for diamond index at the optical wavelength near 4μ.

Table 4. Comparison of refractive indexes

Material	n_{val} (Cal.)	n (Ref.)	Variation
Quartz	2.25	2.102	7%
		2.153	5%
Sapphire	3.28	3.060	7%
		3.402	4%
Diamond	2.53	2.36	7%

Table 4 compares our results with the reference values. The calculated n_{val} values for quartz and sapphire are based on the samples with unknown optical axis and the corresponding reference values are between $n_{\perp}$ and $n_{\parallel}$. However, Table 4 shows

a consistency with literature values of about 7%. In general, open resonator and Math CAD computational procedures give a useful method for determining the permittivities of dielectric samples. It is important to point out that t′ should be modified in anisotropic samples. Emert[18] and Bhawalkar[19] have shown that the maximum effect of dielectric anisotropy can be estimated by substituting t" for t′ in Eqs. (3.7) to (3.11) where

$$t'' = (n_{\parallel}^2/n_{\perp}^2)\, t' = (n_{\parallel}^2/n_{\perp}^2)\,[t + w(t)^2/4R(t)] \qquad (3.34)$$

With this change, more accurate measurements of refractive indexes for anisotropic samples may be obtained.

3.7 Measurement of loss tangent in some transparent substances

Loss-tangent measurements are basically dependent on the measured Q values in the resonator. It is desirable that Q_d should be, within an order of magnitude, comparable with Q_0 in low loss materials. If it is not, one should be able to carry out very precise and repeatable Q measurements.

3.7.1 Results

Empirical Q measurements determine $D/\Delta D$ by detecting the half-power points. Our calculated results are based on the data from the experiment performed by Cook *et al.* at 337 GHz. The samples are the same as we used in dielectric permittivity measurements. Figure 7 shows comparative cavity scans for some dielectric samples. The measured values of half-power width are given in Table 5.

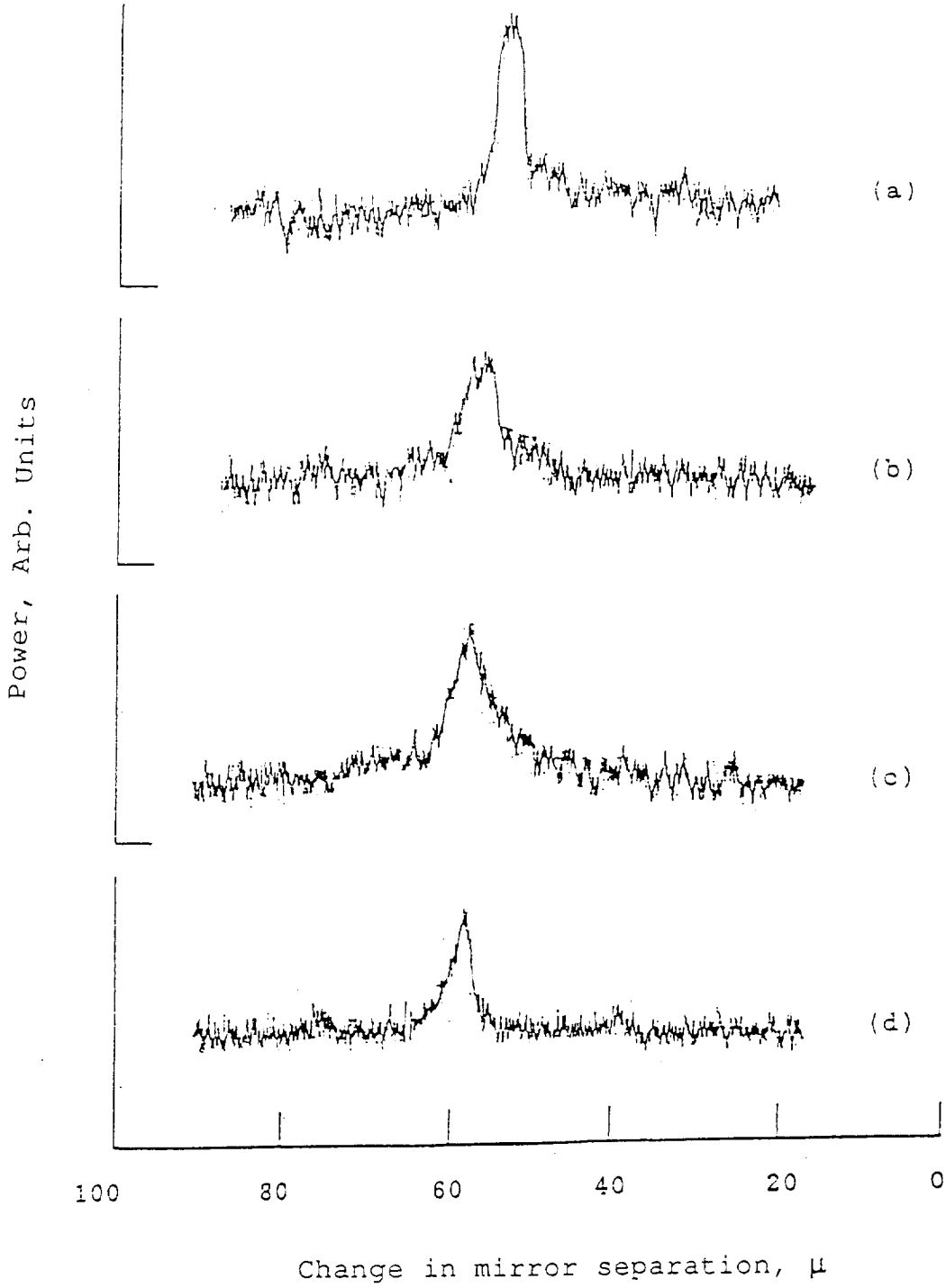

Fig. 7. Sample spectra taken with a scanning hemispherical open resonator for empirical cavity Q measurements
(a) empty (b) loaded with quartz
(c) loaded with diamond (d) loaded with sapphire

Table 5. Q values for the empty and sample-loaded resonator

Sample	D (mm)	ΔD_o[a] (μ)	ΔD_s[b] (μ)	Q_o[c] (10^3)	Q_s[d] (10^3)
Quartz	113.707	1.25	1.50	91	76
Diamond	113.707	1.25	2.25	91	51
Sapphire	113.707	1.25	1.66	91	65

a. Half-power width for the empty resonator

b. Half-power width for the loaded resonator

c. Q-factor for the empty resonator

d. Q-factor for the loaded resonator

Using Eqs. (3.12), (3.14) and (3.15), we calculated the loss tangents shown in Table 6.

Table 6. Loss tangents of Quartz, Diamond and Sapphire

Sample	t (mm)	p (mm)	n reference	Q_s (10^3)	$\tan\delta$ (10^{-3})
Quartz	0.659	0.338	2.153	1716	0.085
Diamond	0.250	0.353	2.36	1347	0.154
Sapphire	0.508	0.352	3.402	280	0.654

The resonator cavity is extremely sensitive to small misalignments in either mirror. Therefore, it is critical that the translational stage be firmly mounted in such a manner

that forward and backward movement will not misalign the cavity over multiple runs. This misalignment presented itself in this experiment because the intervals between the scaled mirror separations shown in Figure 7 are not linear at certain rate of cavity scan. It is estimated that errors in determination of ΔD were about 10% so that the uncertainty in $\tan\delta$ was found to be 25% due to this method of measuring the Q-factor and other losses in the cavity.

3.7.2 Discussion

Mirrors used in the resonator are made from aluminum. Using the measured values of surface resistivity of aluminum found in Table 1, we can obtain a theoretical empty Q-factor from Eq. (1.46). This Q value is about 9.2×10^4 in the resonant length of 113.707 mm. The empty Q-factor Q_o measured by the experiment and shown in Table 5 is then found to agree with the theoretical estimates. We expect to make measurements of Q-factors of magnitudes of about 10^5 to better than 10%.

Except for the uncertainty of this measuring method, another factor affecting the measurement of loss tangent is the sample thickness. It has been shown by Jones (see Ref. 13) that possible errors are minimum when the sample thickness is an integral number of a half wavelength thick. Unfortunately, none of our samples has a thickness like this because of

limited availability. It is expected that the loss tangent of sapphire has the least error since its thickness is closer to a half wavelength than the other two samples.

Although the measurement was somewhat inaccurate due to the problem mentioned above, the use of the resonator in the submillimeter-wave region is a feasible method to measure loss tangent. This is the first demonstrated use of a far-infrared laser as a dependable research tool in this context.

4. Summary

In this work we have extended the derivation of theoretical formulas for Q-factors of open resonators by using scalar theory and Gaussian beam model for small sample. This work is used in determining experimental Q-factors obtained from measurements of metallic surface resistivities and dielectric constants. It is important because these measurements are dependent on the accurate measurement of the cavity Q. To avoid spurious oscillating modes in the resonator, use of a small sample is essential. The modified theory, dealing with the small planar mirror of the open resonator, indicates that the existing theories can still be used if the sample radius is larger than $1.5w_o$.

This work justifies the use of small sample arrangements. Using hole coupling techniques in the open resonator at high frequencies of about 337 GHz with FIR lasers is a new approach in measuring metallic surface resistivities and dielectric constants. Although the response time and sensitivity of the experimental system needs to be improved, it extends applications of the open resonator into the submillimeter-wavelength region.

References

1. J. D. Cook, J. W. Zwart, K. J. Long, V. O. Heinen, and H. Stankiewicz, Rev. Sci. Instrum. **62**, 2480 (1991)
2. J. D. Cook, K. J. Long, V. O. Heinen, and H. Stankiewicz, Rev. Sci. Instrum. **63**, 1 (1992)
3. J. S. Martens, V. M. Hietala, D. S. Ginley, T. E. Zipperian, and G. K. Hohenwarter, Appl. Phys. Lett. **58**, 2543 (1991)
4. R. G. Jones, Electron. Lett. **11**, 545 (1975)
5. A. Maitland and M. H. Dunn, "Laser Physics", Amsterdam, North-Holland, 1969, p. 131
6. H. Kogelnik and T. Li, Proc. IEEE **54**, 1312 (1966)
7. A. Siegman, "Laser", University Science Books, Mill Valley, CA, 1986, p. 734
8. P. Lorrain and D. R. Corson, "Electromagnetic Fields and Waves", Freeman, New York, 1970, p. 439
9. J. D. Jackson, "Classical Electrodynamics", Wiley, New York, 1975, p. 336
10. R. G. Jones, Proc. IEEE **123**, 285 (1975)
11. A. G. Fox and T. Y. Li, Bell Sys. Tech. J. **40**, 480 (1961)
12. A. L. Cullen and P. K. Yu, Proc. Roy. Soc. **A325**, 493 (1971)
13. R. G. Jones and R. J. Cook, Electron. Lett. **11**, 543 (1975)

14. Z. H. Yang, C. W. Lin, and Y. W. Zho,
10th International conference on Infrared and Millimeter Waves, Lake Buena Vista, Fl, Dec. 9-13,
IEEE Cat. No.85CH2204-6, 1985

15. F. Seitz, "Modern Theory of Solids",
McGraw, New York, 1940, Ch.XVII

16. S. Roberts and D. D. Coon,
J. Opt. Soc. Am. **52**, 1023 (1962)

17. V. Camp, V. E. Van Doren, and J. T. Devreese,
Phys. Rev. **B 17**, 2043 (1978)

18. H. Emert, Electron. Lett. **6**, 720 (1970)

19. D. D. Bhawalkar, A. M. Goncharenko, and R. C. Smith,
Br. J. Appl. Phys. **18**, 1431 (1967)

Appendix

Math CAD Program for finding index of refraction

Open Resonator design for hemispherical resonator - λ=wavelength, Ro=mirror radius, modes are TEMplq, d=separation of mirrors in mm.

λ := 0.89011 Ro := 113.82 p := 0 l := 0 q := 254

Find separation of mirrors for resonance of TEMplq mode.

First guess d := 44

Given

$$2\cdot\frac{d}{\lambda}\cdot\pi\cdot(q+1)+\frac{2\cdot p+l+1}{\pi}\cdot\operatorname{atan}\left[\sqrt{\frac{d}{Ro-d}}\right] \qquad d < Ro$$

dval := Find(d) dval = 113.707

n := 2.60 t' := .250 p := .353 t := .250

$$k := 2\cdot\frac{\pi}{\lambda} \qquad d(n,t) := dval - t - p$$

$$w0(n,t) := \left[\frac{2}{k}\cdot\left[d(n,t)+\frac{t}{2}\right]\cdot\left[Ro-d(n,t)-\left[\frac{t}{2}\right]\right]\right]^{.5}$$

$$w1(n,t) := (w0(n,t))\cdot\left[1+\left[\frac{2\cdot t}{k\cdot(w0(n,t))^2}\right]^2\right]^{.5}$$

$$R1(n,t) := t \left[1 + \left[\frac{w0(n,t)}{t}\right]^2\right]^2$$

$$L(n,t) := k\, w0(n,t)^2$$

$$\phi t(n,t) := \operatorname{atan}\left[2 \frac{t}{n\, L(n,t)}\right]$$

$$\phi d(n,t) := \operatorname{atan}\left[\left[\frac{2}{L(n,t)}\right] \left[d(n,t) + \frac{t}{n^2}\right]\right] - \operatorname{atan}\left[\left[2 \frac{t}{n^2 L(n,t)}\right]\right]$$

Given

$$n = -\left[\frac{\tan(n\, k\, t - \phi t(n,t))}{\tan(k\, d(n,t) - \phi d(n,t))}\right]$$

$$t = t' + \frac{w1(n,t)^2}{4\, R1(n,t)}$$

$$\begin{bmatrix} nval \\ tval \end{bmatrix} := \text{Find}(n,t)$$

$$nval = 2.53$$

$$tval = 0.253$$

$$ERR = 4.885 \cdot 10^{-15}$$